Article ID: 1003－6326(2004)05－0858－06

Formation and crystallization of Zr-Ni-Ti metallic glass①

LIU Xiong-jun(刘雄军)[1], HUI Xi-dong(惠希东)[1],
JIAO Jian-ting(焦建廷)[2], CHEN Guo-liang(陈国良)[1]
(1. State Key Laboratory of Advanced Metals and Materials,
University of Science and Technology Beijing, Beijing 100083, China;
2. Shandong Water Engineering Co., Ltd., Ji'nan 250013, China)

Abstract: The metallic $Zr_{65}Ni_{25}Ti_{10}$ (mole fraction, %) glass has been fabricated by a single roller melt-spinning method. The glass forming ability(GFA) and thermal stability of the $Zr_{65}Ni_{25}Ti_{10}$ melt-spun ribbons were investigated by using X-ray diffraction(XRD) and differential scanning calorimetry(DSC) in the mode of continuous heating. It is shown that the reduced glass transition temperature (T_{rg}) is 0.506 and the supercooled liquid region (ΔT_x) is 30 K. Two exothermic peaks were observed in the DSC curves of the as-quenched ribbon, which indicates that the crystallization process undergoes two different stages. The phase transformation during the isothermal annealing was investigated by X-ray diffraction(XRD) and transmission electronic microscope(TEM). It is observed that the metastable FCC Zr_2Ni(Fd3m, a = 12.27 Å) precipitated while annealing in the suppercooled region(615 K) and the stable BCT Zr_2Ni(I4/mcm, a= 6.499 Å, c= 5.270 Å) precipitated while annealing at higher temperature(673 K or 723 K). The crystallines are on nanoscale, with grain size of 15－30 nm. The reason for the precipitation of the different structural Zr_2Ni from the glassy matrix under different annealing conditions was discussed based on the concept of multi-component chemical short range order(MCSRO).

Key words: metallic glass; glass forming ability; crystallization; structural transformation; Zr-Ni-Ti
CLC number: TG 139.8 **Document code:** A

1 INTRODUCTION

Most of the icosahedral quasicrystal phases (i-phase) reported are metastable phases which can be formed by rapid quenching techniques. However, thermodynamically stable i-phase $Zr_{41.5}Ti_{41.5}Ni_{17}$ (mole fraction, %) was discovered by Kelton et al[1] in Zr-Ti-Ni alloy system. Therefore the Zr-Ti-Ni ternary alloy system has been studied extensively. Phase stability and transformation of the i-phase in $Zr_{41.5}Ti_{41.5}Ni_{17}$ alloy were investigated by YI et al[2]; Majzoub, Hennig and their co-workers[3, 4] have developed the structural modeling of the Ti-Zr-Ni quasicrystal and its approximants using experimental method combined ab initial relaxation studies; the properties of Zr-Ti-Ni quasicrystals have also been studied. The microhardness value(3.6 GPa) of Ti-Zr-Ni nanoquasicrystal phase is three times as the usual hardness of the micron-sized quasicrystals in the Al-based quasicrystals[5]. Superconductivity of Ti-Zr-Ni alloys containing quasicrystals was found by Azhazha et al[6]. Another attractive feature of Zr-Ti-Ni system for the application is that the alloys are hopeful to be novel and high-quality hydrogen storage material in the future. Amorphous Zr-Ni is capable of storing hydrogen with [H]/[M] of 1.6[7] (where [H] and [M] are the atom number of hydrogen and metal, respectively). Viano et al[8] have determined that the i-phase storing hydrogen amounts up to [H]/[M] = 1.6 in $Zr_{38}Ti_{45}Ni_{17}$ alloy. An electrochemical method was used in hydrogenate Ti-based quasicrystals and the result shows that the maximum value of absorbing hydrogen of $Zr_{38}Ti_{45}Ni_{17}$ quasicrystals can reach 1.9[3].

From the above investigation on Zr-Ti-Ni alloys, we can see that most works were concentrated on the quasicrystals in this kind of alloy. Few researches were focused on the amorphous. Molokanov et al[9] have determined that the amorphous and quasicrystals formation ranges in the rapidly solidified Zr-Ti-Ni alloys, and the glass forming ability(GFA) was estimated from critical amorphous ribbon thickness(the maximum value is 680 μm). YI et al[10] has studied the nano-crystallization of $Zr_{47}Ni_{30}Ti_{23}$ amorphous ribbons and indicated that it was possible to attain nanocrystal-amorphous composites through the controlled crystallization of the amorphous. In this paper, $Zr_{65}Ni_{25}Ti_{10}$ alloy is designed successfully and

① **Foundation item:** Project(50171006) supported by the National Natural Science Foundation of China; project(2001AA331010) supported by the Hi-tech Research and Development Program of China; project(G2000067201-3) supported by the National Basic Research Program of China; project(H020420030320) supported by the Major Program of Science and Technology of Beijing
Received date: 2004－03－01; **Accepted date:** 2004－05－03
Correspondence: LIU Xiong-jun, PhD candidate; Tel: +86-10-62332169; E-mail: luckyxjliu@163.com

its full amorphous ribbons are fabricated, the crystallization process and phase transformation of the as-quenched ribbons under different annealing conditions are investigated.

2 EXPERIMENTAL

The glass forming alloys with a nominal composition of $Zr_{65}Ni_{25}Ti_{10}$ were prepared by arc melting mixture of pure zirconium (99.9%, mass fraction, the same below), titanium (99.9%) and high-purity nickel (99.999%) under a Ti-gettered pure argon atmosphere. The alloy ingots were remelted several times to ensure homogeneity. The master ingots were surface-polished, broken into small pieces and put into quartz tubes and then melted by induction at high vacuum ($(4.5-5.0)\times10^{-3}$ Pa). Amorphous ribbons with a cross-section of about 0.06 mm × 5 mm were produced by the vacuum single-roller melt spinning technique (the diameter of copper roller and line velocity are 200 mm and 30 m/s, respectively). X-ray diffraction (Cu K_α, Philips APD-10) and transmission electronic microscope (TEM, JEOL 2000FX, operating at 160 kV) were exploited in order to examine the amorphicities of ribbons. The glass transition temperature (T_g) and the onset crystallization temperature (T_{x1}) of samples were estimated by means of differential scanning calorimetry (DuPont DSC2010). The quenched ribbons were annealed isothermally under different conditions, and the particular parameters of annealing treatment are shown in Table 1. XRD and TEM techniques were used to investigate the annealed samples in turn. TEM samples were prepared electrolytically by twinjet polishing at 240 K in a mixing solution of 90% methanol and 10% (volume fraction) perchloric acid.

Table 1 Condition of annealing process

Temperature/K	Time/min	Vacuum/(10^{-3} Pa)
615	2 5 15	4.0
673	5 15	4.0
723	15	4.0

3 RESULTS AND DISSCUTION

3.1 Glass forming ability (GFA) and thermal stability

Fig. 1 shows the ternary phase diagram of Zr-Ni-Ti[11] which shows that the composition of the alloy locates between α-Zr(Ti) solid solution and Zr_2Ni phase. Equilibrium phases in the $Zr_{65}Ni_{25}Ti_{10}$ alloy are mainly Zr_2Ni phase and a small amount of α-Zr(Ti) solid solution.

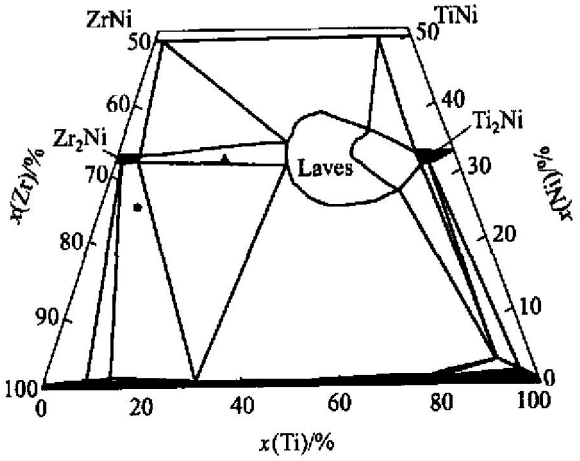

Fig. 1 Partial isothermal section of Zr-Ni-Ti ternary system at 973 K
▲ —Pseudo-binary eutectic;
● —Composition of $Zr_{65}Ni_{25}Ti_{10}$ alloy

During rapid quenching on the melt spinner, the formation and growth of the crystalline phases from liquid is completely suppressed. The structure of liquid melts was frozen and amorphous phase was formed, which can be confirmed by XRD and TEM analysis. XRD pattern of the as-melt spun ribbon is a typical amorphous feature as shown in Fig. 2, which has a diffused halo and not any other acute diffract peaks. Fig. 3(a) shows the TEM bright image of the $Zr_{65}Ni_{25}Ti_{10}$ as-quenched ribbon. It can be seen obviously that no crystalline phase exist in the image. Fig. 3(b) is the corresponding selected area diffraction pattern (SADP) of the sample, which shows the diffused diffraction rings corresponding to typical electron diffraction pattern of amorphous. These results confirmed that the $Zr_{65}Ni_{25}Ti_{10}$ ribbon is of full amorphous structure.

Essentially, the glassy state of alloy is the

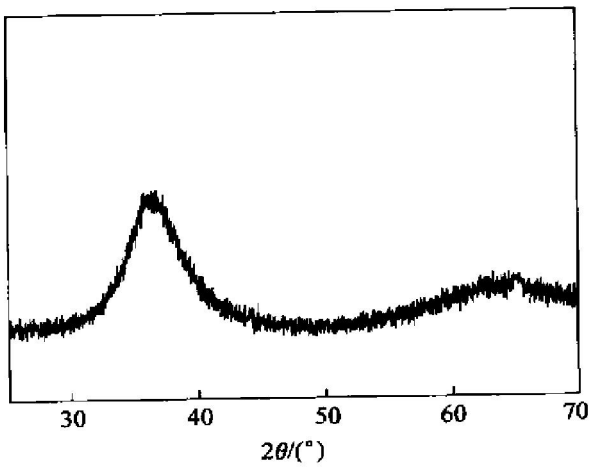

Fig. 2 XRD pattern of as-melt spun ribbon $Zr_{65}Ni_{25}Ti_{10}$

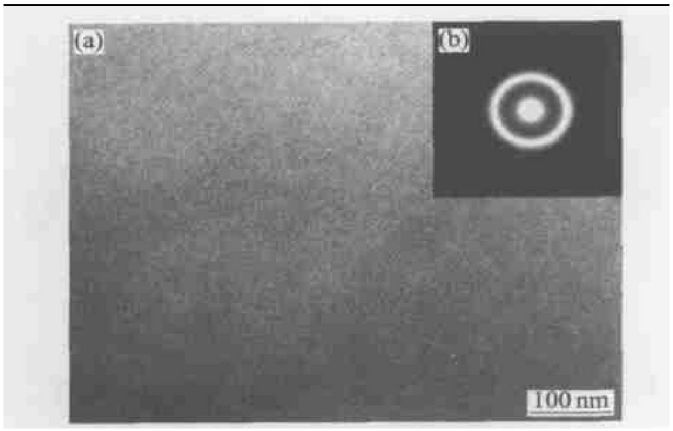

Fig. 3 TEM bright image(a) and corresponding SADP of $Zr_{65}Ni_{25}Ti_{10}$ melt-spun ribbon(b)

frozen structure of liquid melts. When the alloy melts suppercooled under its melting temperature(T_m), the value of structural relaxation time(τ) of system will be less than the reciprocal of cooling rates dT/dt, which makes the system on metastable state with no precipitation of crystalline. When the alloy melt was undercooled continuously, its viscosity coefficient(η) or τ will increase sharply. Upon τ being up to a critical value(τ_g), which results in non-equilibrium in the limited time, namely, the configuration of atoms was frozen into nonequilibrium metastable state with glassy structure. This shows that the GFA of alloy system is strongly correlative to η, enhancing the GFA of alloys with increasing η. Till now many criteria[12-14] or empirical rule[15] of the evaluation of GFA are all correlative to this in essence. Turnbull[12] has suggested the reduced glass transition temperature T_{rg}(T_g/T_l, where T_g and T_l are the glass transition temperature and liquidus temperature, respectively) is an important parameter for the evaluation of GFA. According to his analysis, the liquid with T_{rg} larger than 2/3 could only crystallize within a very narrow temperature range and the homogeneous nucleation rate can not be measured practically, i.e. could form amorphous phases. However, it is also true that the values of T_{rg} for the present bulk metallic glass forming alloys are consistently less than the value of 2/3, except for $Pd_{40}Ni_{10}Cu_{20}P_{40}$ alloy[16] which has a slightly higher value of 0.690. At the same time, Lu et al[17] have found out that T_{rg} for the present bulk metallic glass forming alloys are all larger than 0.5. Fig. 4 shows the continuous heating with 40 K/min DCS curve of the $Zr_{65}Ni_{25}Ti_{10}$ metallic glass. It is seen that the T_{rg}= 0.506(where T_g is 601 K and T_l is 1 187 K). In this work, the maximum thickness value of full amorphous alloy is about 80 μm. Therefore, we have reasons to believe that it is possible to increase the GFA if some new elements are added into the primary alloy.

Generally, one estimates the thermal stability of metallic glass alloys using suppercooled liquid regions ΔT_x(= T_{x1} − T_g, where T_{x1} and T_g are the onset crystallization temperature and glass transition temperature, respectively), considering the greater value of ΔT_x corresponds to the better thermal stability. The ΔT_x= 30 K(where T_g= 601 K and T_{x1}= 631 K) of the $Zr_{65}Ni_{25}Ti_{10}$ as-melt spun ribbon can be obtained from Fig. 4. It indicates that the thermal stability of this metallic glass alloy is comparatively better, which is confirmed by the following annealing experiments. The sample maintains the glassy structure after annealing for 2 min in suppercooled region (615 K).

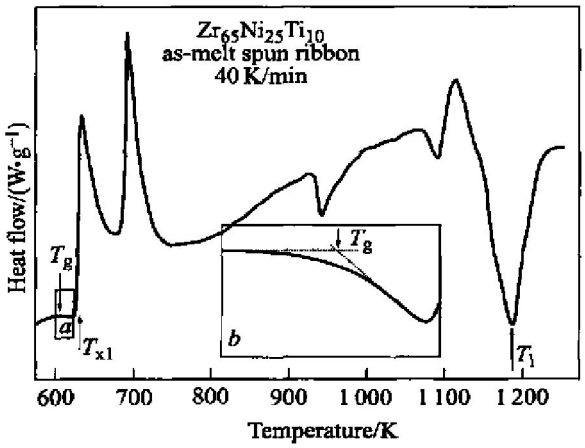

Fig. 4 DSC curve of as-melt spun ribbon $Zr_{64}Ni_{25}Ti_{10}$
(*b* is amplified region of *a*)

3.2 Crystallization process during isothermal annealing

The crystallization process of metallic glasses is essentially a process of the disordered glassy structure transformation to ordered crystalline structure, with the saltation of some physic and chemical properties including resistivity, elastic module, susceptibility and special heat capacity and so on. Two distinct separable exothermic peaks can be seen from Fig. 4 owing to the exothermic reaction of transition from amorphous to crystal, indicating that the crystallization proceeds through a double different stage mode. Fig. 5 shows the XRD patterns of $Zr_{65}Ni_{25}Ti_{10}$ as-melt spun ribbons annealed under different conditions. The indexed diffraction results indicate that the precipitates from amorphous matrix are mainly metastable FCC Zr_2Ni(Fd3m, a= 12.27 Å), plus a small amount of ω-Zr(P6/mmm, a= 5.327 Å, c= 4.321 Å) solid solution when ribbon isothermally an-

nealed in the suppercooled region(615 K) (as curves (a), (b), (c) shown in Fig. 5); when the ribbon is annealed exceeding the crystallization temperature (673 K) (as curves (d), (e) shown in Fig. 5), the precipitates are mainly stable BCT Zr_2Ni(I4/mcm, a = 6.499 Å, c = 5.270 Å) and a small amount of α-Zr($P6_3/mmc$, a = 3.23 Å, c = 5.14 Å) solid solution as well as some unidentified phase; when the ribbon annealed at higher temperature(723 K) (as curves (f) shown in Fig. 5), there are no new phases precipitated but the amount of α-Zr solid solution is more than that at 673 K.

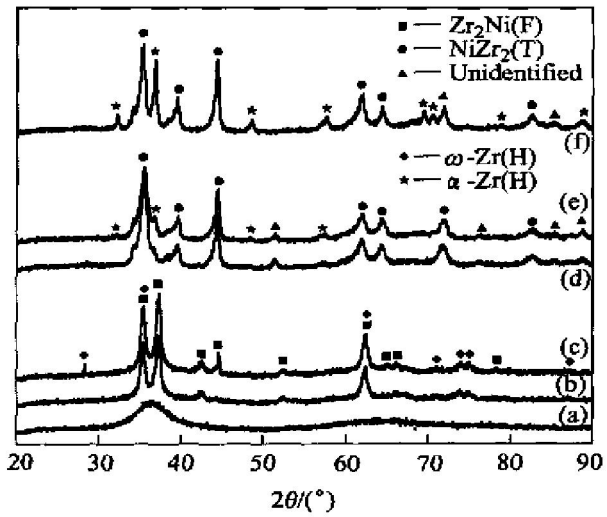

Fig. 5 XRD patterns of $Zr_{65}Ni_{25}Ti_{10}$ as-melt spun ribbons annealed under different conditions
(a) —615 K, 2 min; (b) —615 K, 5 min; (c) —615 K, 15 min; (d) —673 K, 5 min; (e) —673 K, 15 min; (f) —723 K, 15 min

The formation and structure of precipitates are mostly dependent on the atom diffusion and the interfacial energy between precipitates and amorphous matrix during the metallic glasses annealed under isothermal annealing conditions. The atom diffusion is related to the temperature, pressure, relative size of atoms, chemical properties and concentration of constitutes, and the chemical interaction of the clusters in the amorphous, etc. On the other hand, the interfacial energy between precipitates and amorphous matrix is mainly determined by the structural differences between the precipitated phases and matrix. The more close the structure of new crystallization phases to the amorphous structure are, the less the interfacial energies are and the easier the crystallization nucleation. Chen and Hui et al[18, 19] have proposed that there are many multicomponent chemical short-range order(MCSRO) domains with the composition similar to the corresponding well-defined compounds or crystalline phases as its crystalline counterpart co-exist in the metallic glass, and verified that the F-Zr_2Ni and T-Zr_2Ni MCSRO domains existed in the Zr-based bulk metallic glass by experimental observation. These MCSRO can act as nucleus of no-classic nucleation and diffusion controlled nucleation[20]. Matsubara et al[21] have investigated the short-range order(SRO) and the structure of crystalline phase in $Zr_{60}Al_{15}Ni_{15}$ metallic glass by analyzing radial distribution function(RDF). The results shows that the coordination numbers(CN) of Zr-Ni are not different after annealing, implying that the structural difference between short-range order(SRO) and the precipitated compound phases of $Zr_{60}Al_{15}Ni_{15}$ metallic glass is very small. For the present alloy, when annealed at lower temperature(615 K), the diffusion of nickel atom can not proceed, so the precipitates are mainly metastable FCC Zr_2Ni phase, because the FCC Zr_2Ni is more close to the amorphous matrix structure and its growth does not need long path diffusion of nickel atom as well as the interfacial energy is less. When annealed at higher temperature(673 K, 723 K), the T-Zr_2Ni MCSRO domains of metallic matrix will become the nucleus of no-classic nucleation and diffusion controlled nucleation and grow into BCT Zr_2Ni phases, and there are local Zr-riched zones in the residual amorphous matrix because of the nickel atomic diffusion. Therefore, the α-Zr solid solution precipitates from the amorphous matrix, and the nickel atomic diffusion increases with the rising annealing temperature, which is the chief reason why the quantity of α-Zr solid solution at 723 K is more than that at 673 K. The metastable FCC Zr_2Ni phases precipitated from amorphous matrix will transform into stable BCT Zr_2Ni phase. It is also possible that F-Zr_2Ni MCSRO domains in the matrix directly form BCT Zr_2Ni phases by the micromechanism of cluster deposition[22].

3.3 Formation of nanocrystalline

From Fig. 5, it can be seen that the XRD patterns of the precipitates are broadened for the crystalline being fine. The average grain size(L) of crystallized phases under different annealing conditions can be estimated from the maximum half-width(β) of the X-ray reflections using Scherrer formula[23]

$$\beta = \frac{K\lambda}{L\cos\theta} \quad (1)$$

where λ is the radiation wavelength and θ the diffraction angle, and K = 0.94. The calculated results shown in Table 2 indicate that the nanocrystallines precipitate from the amorphous matrix after annealing. The average grain size of the crystallized phases is 15 ~ 30 nm, which is consistent with the TEM results as shown in Fig. 6, illustrating that the calculated results is reliable.

To obtain nanoscale structure, the crystallization process should proceed with the largest nucleation

Table 2 Average grain size of crystallized phases under different annealing conditions based on Eqn. (1)

Annealing condition	2θ/(°)	β/rad	λ/nm	L/nm	$\overline{L}$/nm
615 K, 15 min	35.452	0.005 518	0.154 056	26.563 13	26.183 75
	37.313	0.005 526	0.154 056	26.556 1	
	62.387	0.005 912	0.154 056	25.432 02	
673 K, 15 min	35.513	0.009 139	0.154 056	16.038 49	15.008 3
	39.277	0.011 353	0.154 056	12.945 64	
	61.885	0.009 367	0.154 056	16.040 79	
723 K, 15 min	35.322	0.005 326	0.154 056	27.513 8	29.322 26
	44.371	0.003 702	0.154 056	39.865 63	
	61.838	0.007 298	0.154 056	20.587 36	

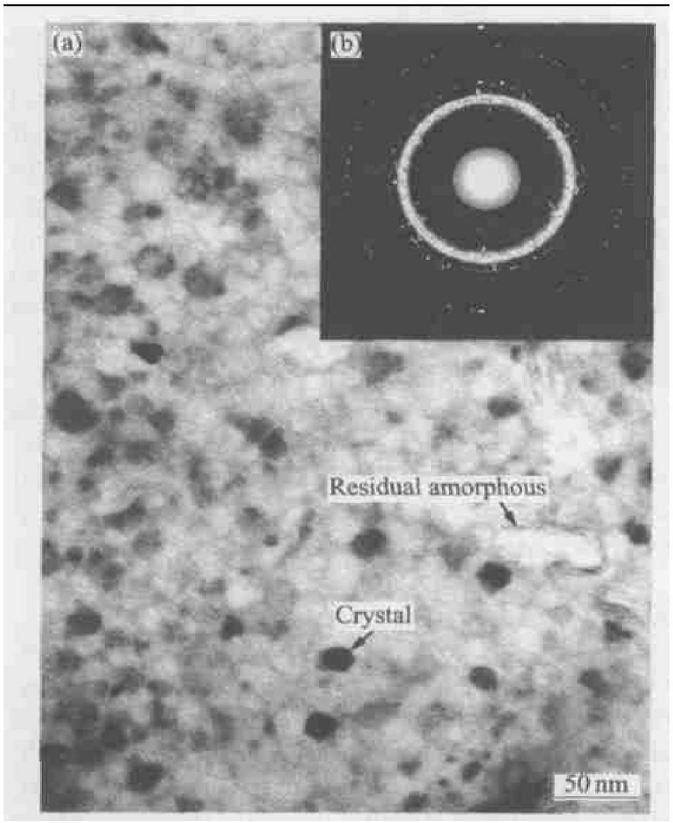

Fig. 6 Microstructure(a) and corresponding SADP(b) for as-melt spun ribbon glass alloy $Zr_{65}Ni_{25}Ti_{10}$ after annealed at 615 K for 15 min

rate and the lowest crystal growth. According to the classic nucleation and growth theory, the stable nucleation of homogeneous nucleation I_n is given by

$$I_n = I_0 \exp\left(-\frac{\Delta G_c}{RT}\right) \exp\left(-\frac{E_n}{RT}\right) \quad (2)$$

where I_0 is a constant, E_n is active energy of nucleation and ΔG_c is the free energy for critical nucleus formation, which is a function of temperature and mostly comprised of interfacial energy of nucleation. The ΔG_c decreases with the lowering interfacial energy. In this work, there are many MCSRO domains in the $Zr_{65}Ni_{25}Ti_{10}$ amorphous ribbon and these MCSRO domains can act as nucleation site, and therefore the interfacial energy of precipitates is very low, resulting in the small ΔG_c. Consequently, the nucleation rate is extraordinary high. It is observed that a maximum value of nucleation rate appears with temperature variation during the crystallization process of Fe-Si-B metallic glass[22], and this phenomenon was found in other alloy systems[24]. The classic nucleus growth theory shows that the growth rate increases with temperature rising. But there has a temperature range with high nucleation rate and low growth rate, which is of advantage for obtaining the fine grains[22]. The temperature range also presents in $Zr_{65}Ni_{25}Ti_{10}$ metallic glass, so nanocryatallines can be obtained. It can be presumed from Table 2 that the temperature range with high nucleation rate and low growth rate is near 673 K, because the grain size of precipitates is the smallest about 15 nm when the samples annealed at 673 K. So it is possible to achieve nanocrystalline materials through the controlled crystallization process of this metallic glass. The further work is being conducted.

4 CONCLUSIONS

1) The glass transition temperature T_g of the $Zr_{65}Ni_{25}Ti_{10}$, onset crystallization temperature T_{x1}, reduced glass transition temperature T_{rg} and supper-cooled liquid region ΔT_x are 601 K, 631 K, 0.506 and 30 K, respectively.

2) Crystallization process of the $Zr_{65}Ni_{25}Ti_{10}$ metallic glass undergoes two different stages during the isothermal annealing. The microstructure transformation is from amorphous to amorphous matrix plus metastable FCC Zr_2Ni(Fd3m, a= 12.27 Å) and ω-Zr(P6/mmm, a= 5.327 Å, c= 4.321 Å) solid solution, then to stable BCT Zr_2Ni(I4/mcm, a= 6.

499 Å, c = 5.270 Å) plus α-Zr ($P6_3/mmc$, a = 3.23 Å, c = 5.14 Å) solid solution as well as a small amount of unidentified phases.

3) The grain size of crystallized phases is 15 – 30 nm. It is possible to obtain nanocrystalline materials through the controlled crystallization process of this metallic glass.

REFERENCES

[1] Kelton K F, Kim W J, Stroud R M. A stable Ti-based quasicrystal [J]. Appl Phys Lett, 1997, 70(24): 3230 – 3232.

[2] Yi S, Kim D H. Stability and phase transformations of icosahedral phase in a 41.5Zr41.5Ti17Ni alloy [J]. J Mater Res, 2000, 15(4): 892 – 897.

[3] Majzoub E H, Kim J Y, Hennig R G, et al. Cluster structure and hydrogen in Ti-Ni-Zr quasicrystals and approximants[J]. Mater Sci Eng A, 2000, A294 – 296: 108 – 111.

[4] Hennig R G, Majzoub E H, Carlsson A E, et al. Structural modeling of the Ti-Zr-Ni quasicrystal[J]. Mater Sci Eng A, 2000, A294 – 296: 361 – 365.

[5] Shaz M A, Mukhopadhyay N K, Mandal B K, et al. Synthesis and microhardness measurement of Ti-Ni-Zr nanoquasicrystalline phase [J]. J Alloys Compounds, 2002, 342(1 – 2): 49 – 52.

[6] Azhazha V, Grib A, Khadzhay G, et al. Superconductivity of Ti-Zr-Ni alloys containing quasicrystals[J]. Phys Lett A, 2002, 303(1): 87 – 90.

[7] Kirchheim R, Sommer F, Schluckerbier G. Hydrogen in amorphous metals(Ⅰ)[J]. Acta Metall, 1982, 30(6): 1059 – 1068.

[8] Viano A M, Stroud R M, Gibbons P C, et al. Hydrogenation of titanium-based quasicrystals[J]. Phys Rev B, 1995, 51(17): 12026 – 12029.

[9] Molokanov V V, Chebotnikov V N. Quasicrystals and amorphous alloys in Ti-Zr-Ni system: glassforming ability, structure and properties[J]. J Noncrystal Solids, 1990, 117/118: 789 – 792.

[10] Yi S, Kim W T, Kim D H, et al. Development of nanocrystals in an amorphous alloy $Zr_{47}Ni_{30}Ti_{23}$[J]. J Mater Sci, 2001, 36(21): 5101 – 5104.

[11] Villas P, Prince A, Okamoto H. Handbook of Ternary Alloy Phase Diagrams[M]. OH. USA: ASM. International. Material Parks, 1995. 13062 – 13063.

[12] Turnbull D. Under what conditions can a glass be formed[J]. Contemp Phys, 1969, 10: 473 – 488.

[13] Davis H A, Lewis B G. A generalized kinetic approach to metallic glass formation[J]. Scripta Met, 1975, 9(10): 1107 – 1112.

[14] Lu Z P, Liu C T. A new glass-forming ability criterion for bulk metallic glass[J]. Acta Mater, 2002, 50(13): 3501 – 3512.

[15] Inoue A. Stabilization of metallic supercooled liquid and bulk amorphous alloys[J]. Acta Mater, 2000, 48(1): 279 – 306.

[16] Nishiyama N, Inoue A. Flux treated Pd-Cu-Ni-P amorphous alloy having low critical cooling rate[J]. Mater Trans JIM, 1997, 38(5): 464 – 472.

[17] Lu Z P, Tan H, Li Y, et al. The correlation between reduced glass transition temperature and glass forming ability of bulk metallic glasses[J]. Scripta Mater, 2000, 42(7): 667 – 673.

[18] Chen G L, Hui X D, Fan S W, et al. Concept of chemical short range order domain and the glass forming ability in multicomponent liquid[J]. Intermetallics, 2002, 10(11 – 12): 1221 – 1232.

[19] HUI Xi-dong, YAO Ke-fu, CHAO Kou-hong, et al. Chemical short-range order domain in bulk amorphous alloy and predication of glass forming ability[J]. Science in China, 2003, 46E(6): 581 – 592.

[20] Chen G L, Hui X D, Kou H C, et al. The problem about nonclassic nucleation theory and liquid multi-component chemical short range order[J]. Progress in Natural Science, 2003, 13(10): 1022 – 1030. (in Chinese)

[21] Matsubara E, Waseda Y. Structural studies of new metallic amorphous alloys with wide supercooled region [J]. Mater Trans JIM, 1995, 36(7): 883 – 889.

[22] LU K. Phase transformation from an amorphous alloy into nanocrystalline material [J]. Acta Metall Sin, 1994, 30B(1): 1 – 21. (in Chinese)

[23] Fan X. X-Ray Diffraction of Metals[M]. Beijing: China Machine Press, 1998. 103 – 104. (in Chinese)

[24] LU K. Crystallization and Micro-Mechanism of Amorphous Alloys[D]. Shenyang: Institute of Metal Research of Chinese Academy of Sciences, 1989. (in Chinese)

(Edited by LONG Huai-zhong)